Characterization of Robust Carrier Phase Tracking Techniques under Ionosphere Scintillation Scenarios

Teresa Ferreira, Rui Sarnadas
GMV

Jordi Vilà-Valls, Jose A. López-Salcedo, Gonzalo Seco-Granados
Dept. of Telecommunication and Systems Engineering
Universitat Autònoma de Barcelona (UAB)
08193 Bellaterra, Barcelona (Spain)

Paolo Crosta, Roberto Prieto Cerdeira, Francesca Zanier
European Space Agency (ESA)

***Abstract*—Ionospheric scintillations are known to affect both the magnitude and the phase of the incoming GNSS signal. These phase variations are typically synchronized with a deep fade of the signal level, that could lead to the occurrence of cycle slips (phase jumps), errors in the data demodulation and ultimately loss of lock. These effects have an impact not only on accuracy, but also availability, continuity and integrity. This particular aspect is of critical importance since ionospheric scintillations have been identified as one of the causes for integrity faults that need to be detected in safety critical applications. At receiver level, this can be tackled by the use of robust tracking techniques. In particular, the impact on carrier phase tracking is very important as it is more prone to loss of lock, and it is often used to smooth the code measurements, carrier aiding or even Doppler/user dynamics estimation. Moreover, it is through the impact on phase estimation that the data demodulation capability can be assessed, as well as different applications such as ionospheric characterization. This study assesses the behavior of robust carrier phase tracking techniques using both simulated and real data for the ionospheric scintillations. Finally, it introduces an innovative technique and discusses its potential benefits.**

Keywords—GNSS receiver; tracking loops, robustness; ionospheric scintillations

I. INTRODUCTION

Observed scintillation activity is characterized by a considerable spatial and temporal variability, which depends on factors such as the frequency, zenith angle or angle between the ray path and the Earth's magnetic field. The effect of these factors can be accurately defined based on scintillation theory. However, scintillation dependencies on local time, season, solar and magnetic activity have a stochastic character, meaning that there is no unique relationship between the strength and/or occurrence of scintillation and the particular agent. That is why it is so difficult to forecast the occurrence of scintillations, and therefore predict the impact of ionospheric disturbances on radio, communication, navigation or positioning systems. Various models of scintillation have been developed to describe scintillation levels and therefore assist in mitigating and/ or characterizing this effect.

In this study, both simulated and real data will be used to assess the impact of ionospheric scintillations at the receiver level. Simulated data was obtained with the Global Ionospheric Scintillation Model (GISM), and real data is available thanks to the measurements collected in Cabo Verde in the scope of the MONITOR project, [1], [2].

The performance of selected robust carrier tracking techniques in different ionospheric scintillation conditions is assessed with emphasis on carrier phase tracking. For this purpose, the GNSS receiver tracking stage is implemented in a flexible platform, with a bit-true approach, to process the raw data.

II. ROBUST TRACKING TECHNIQUES

In terms of tracking techniques, the platform used in this study consists of a standard DLL coupled to three different carrier phase tracking techniques: a conventional phase-locked loop (PLL), an adaptive Kalman filter (AKF) and an innovative Kalman filter-based solution (KF-AR).

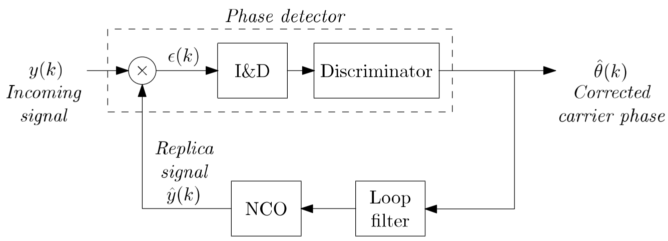

Fig. 1. Block diagram of the conventional PLL.

The conventional PLL depicted in Fig. 1 is the most widely adopted technique in current GNSS receivers, and thus it will be used as a reference technique in the present work. It consists of a closed-loop architecture composed of three constituent blocks: a phase discriminator, which is in charge of providing output measurements that, on average, are proportional to the carrier error to be compensated; a loop filter, which is a low pass filter that smooths the variability due to thermal noise at the discriminator output; and finally a numerically-controlled oscillator (NCO) for generating the corresponding local carrier replica according to the corrections imposed at the loop filter output.

Robust carrier tracking techniques will be represented here by two different variations of Kalman filters. The first one, referred herein as adaptive Kalman filter (AKF) consists on the coupling of a conventional Kalman filter with a method for adaptively estimating the covariance of the measurements noise. In this way, the Kalman filter can keep track of abrupt fades in the input signal, and can react by automatically adjusting the Kalman gains, thus improving its noise rejection capability. The second Kalman filter-based technique consists of a conventional Kalman filter that contains an additional state for estimating the scintillation random process. This is done by assuming that scintillation can fairly be modeled by an autoregressive random process of first order, AR(1), and thus the resulting technique is referred as KF-AR [5].

Thanks to this assumption on the statistical properties of the scintillation time series, tracking of scintillation is possible by incorporating the AR(1) recursion into the Kalman formulation. As any other AR(1) random process, scintillation can be characterized by a single filtering gain, and some white Gaussian noise with a given power. These two parameters (filtering gain and power) need to be determined either by having some a-priori information on the type of scintillation to be processed, or by processing real scintillation time series and then doing some calibration or tuning adjustments to the filter.

Apart from these specific features of both robust techniques proposed herein (i.e. AKF and KF-AR), they share a common closed-loop architecture shown in Fig. 2. As can be seen, this is the conventional Kalman filter architecture where the Kalman gains $\boldsymbol{K}_k$ are in charge of adapting the equivalent loop bandwidth (in particular for the AKF, where the noise covariance is permanently estimated and updated). The transition matrix $\boldsymbol{F}$ contains a second-order modeling of the carrier dynamics (i.e. phase, frequency and frequency rate) and for the KF-AR, an additional term is added to this matrix to incorporate the AR(1) filtering gain for the scintillation time series. This state-space formulation is consistent with a Kalman state vector composed of phase, frequency and frequency rate (for the AKF) and additionally, scintillation phase (for the KF-AR only) [5].

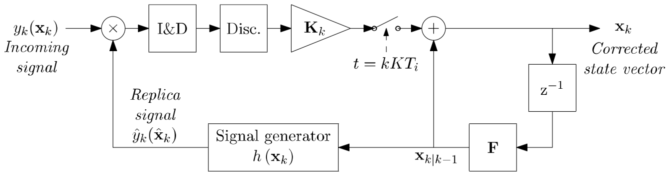

Fig. 2. Block diagarm of a Kalman filter-based carrier tracking loop.

As can be seen, this innovative KF-AR approach allows the receiver to separate the phase contribution due to the user dynamics from the phase contribution due to the random scintillation disturbance. As a result, since the scintillation phase is actually estimated by the KF-AR, it provides an additional and valuable output signal that can be used for scientific applications, atmospheric surveillance and scintillation monitoring purposes.

III. TEST ENVIRONMENT

A. *Test Platform*

The platform used in these tests is depicted in Fig. 3.

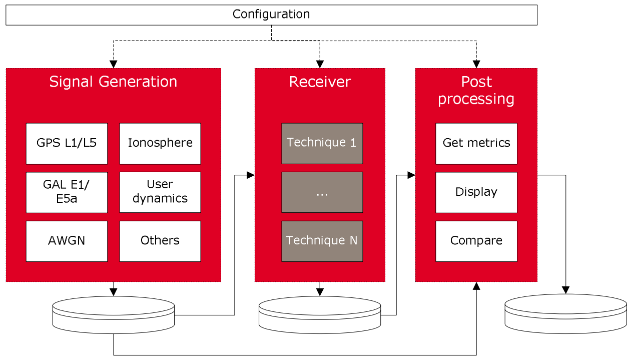

Fig. 3. Test Platform Overview

The platform consists of three modules:

- - Signal Generation

The Signal Generation module generates IF samples according to configurable error sources such as user dynamics and noise. In this study, the generated signal is affected by ionospheric scintillation, whose data series are read from file. These files are obtained from the GISM model and further detailed in the next section. For real data, this module is not used since the receiver module uses the data directly from file.

- - Receiver

The Receiver module implements GNSS receiver tracking loops and it supports different techniques for carrier phase tracking, namely a standard PLL (fully-configurable), an AKF and the KF-AR techniques described in the previous section. The receiver module can be ran directly with IF signal samples from an external file and it is implemented in an efficient way so that, depending on the number of channels configured, it can run faster than real time. This feature was used when running the real data collected with a bit grabber.

- - Post Processing

The Post-Processing module contains different libraries to post-process the results, computing relevant metrics and displaying them in a user-friendly manner.

B. Data Sets

Two types of data sets with ionospheric scintillations are used in this study: simulated data and real data.

Simulated Data

The simulated data consists of time series with ionospheric scintillations generated with the GISM model, described in [3]. The GISM has been accepted as a reference for scintillation evaluations. This model is based on a multiple phase screen technique and it is driven by an electron density climatological model (NeQuick) underneath. The ionospheric scintillations are characterized by the intensity fluctuations given by the scintillation index, S4, and the standard deviation of the phase scintillations. The GISM is able to generate complex time-series of ionospheric scintillations for a given geometry, location, time, date and solar flux.

The data time series used in this study are depicted in Fig. 4 and Fig. 5: they are 100 seconds long and sampled at 10 ms.

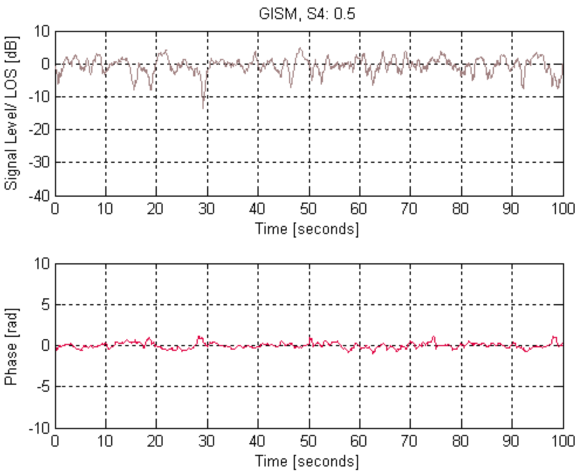

Fig. 4. Simulated Data with GISM for S4=0.5

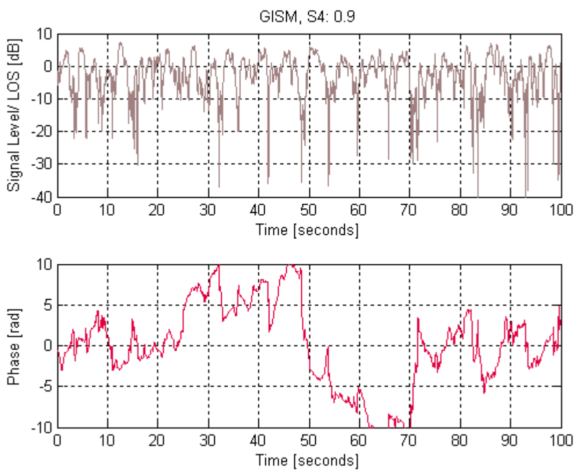

Fig. 5. Simulated Data with GISM for S4=0.9

It can be seen that the phase largest disturbances are synchronized with deep fades of the signal level. These fades have an effect of amplifying the noise level (with respect to the carrier) and can lead to cycle slips (phase jumps), errors in the data demodulation and ultimately loss of lock since the error can be amplified and eventually disturb the code tracking loop as well.

Real Data

Real data was collected in Sal Island, Cabo Verde, in the frame of the ESA GNSS Evolutions Monitor project [1], [2] with the objective of continuous global ionospheric monitoring. In particular this data was gathered for investigating the effect of scintillations beyond the tracking capabilities of scintillation monitors in the time frame of March-April 2013. The data used herein was collected using a narrowband front end sampled at 5 MHz in the L1 band and a fixed receiver (PolaRxS PRO) with a bit grabber recording the data after the front-end.

The S4 index of some of the satellites in the data is depicted in the following figure.

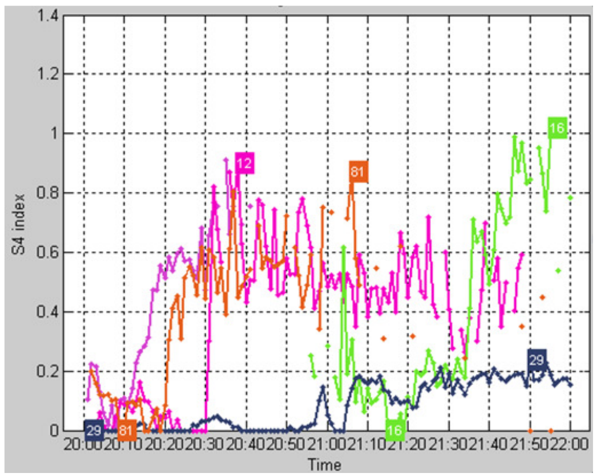

Fig. 6. Scintillation Index of the Signals in the Real Data file

From the full length of data, the 300 seconds from 20:30 to 20:35 was selected since it exhibited a significant scintillation for the Galileo satellite (81) PRN11 which was at an elevation angle of around 30 degrees.

The remaining satellites were finally not included in this study: the satellites with a significant S4 value were very low (e.g. the highest, GPS 12 was at less than 15 degrees) and the other ones (e.g. GPS 29) had very marginal phase variations (i.e. low S4 values).

One important comment regarding real data, is that, although abrupt changes of the signal level are detected, the cause cannot be identified as coming from ionospheric scintillations. For low elevation satellites, for instance, the signal level variations can be due to multipath or distorted antenna patterns at low elevations. At receiver level, the phase disturbances will be surely noted regardless of the cause of the signal level variations, but any assumptions on the behavior of the phenomenon should be carefully considered.

C. *Platform Configurations*

The following table lists the main configuration parameters used to generate the results presented in the next section.

TABLE I. PLATFORM CONFIGURATIONS

Item	Description
PLL	- PLL bandwidth: 10 Hz - PLL order: 2 - PLL discriminator: ATAN2
DLL	- DLL bandwidth: 1 Hz - DLL order: 2 - DLL discriminator: dot product
Others	- Integration time: data symbol (4 ms for Galileo) - Early late spacing: 0.5 chips - User dynamics: fixed - CN0 Estimator: [4]
Post Processing	For real data, carrier is corrected by subtracting the polynomial fit with a 3rd order filter from the carrier estimated by the technique.

IV. RESULTS

The results are presented first for simulated data and then for the real data, focusing on the total carrier phase estimated at the receiver. Finally, the KFAR results are further analyzed in order to assess its capability to identify the scintillation behavior.

A. *Simulated Data*

Results for simulated data are presented hereafter.

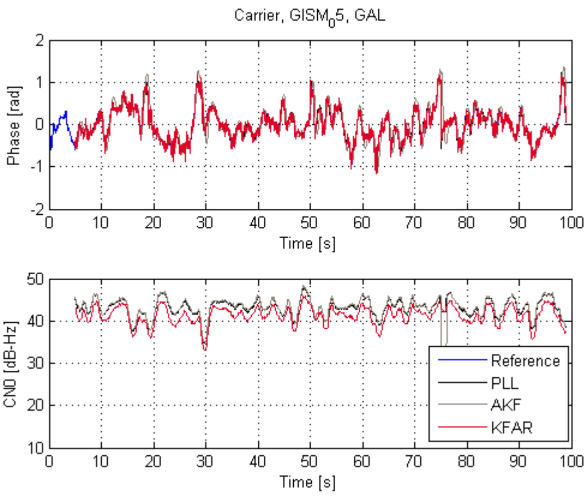

Fig. 7. Results for Galileo, using GISM with S4=0.5

It can be seen that the phase variations caused by this moderate scintillation in Fig. 7 is correctly tracked by all techniques. This is true even for the abrupt changes, aligned with the signal fades – also detected by the platform CN0 estimator. Nevertheless, scintillation fades are not quite deep at all in this case, with maximum values around 10 dB. Therefore, they do not constitute a major issue for the tracking techniques under analysis (even for the conventional PLL).

As for the results for the GISM data series with a scintillation index of 0.9, the total carrier phase is presented in Fig. 8. In this case, scintillation fades are larger, reaching values on the order of 15 dB, and thus leading the working C/N0 to values close to 30 dB-Hz or even less. However, the fall down to this minimum C/N0 is done in a smooth manner, since it takes on the order of 1-2 seconds to reach the minimum value once a deep fade appears. This typically involves hundreds or even thousands of samples at the correlator output, and therefore, the tracking techniques can reasonably keep track, as observed in the upper plot of Fig. 8.

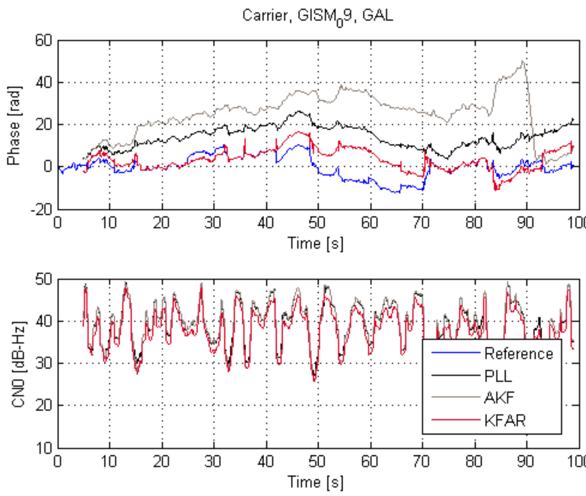

Fig. 8. Results for Galileo, using GISM with S4=0.9

Even though all the techniques follow well the behavior of the phase of the ionospheric scintillations, it can be seen that there is an offset between them, which is a multiple of PI. This happens because the results are not wrapping the phase. Still, looking at this total phase, it seems that the KFAR is still the one closer to the simulated phase, which should be close to zero because no user dynamics are being considered in this simulation. In that sense, the KF-AR shows the smallest phase deviations and thus the more robust performance for this severe scintillation scenario with S4=0.9. Even though the reference PLL also seems to provide an acceptable carrier tracking performance, it exhibits a much larger probability of loss of lock (not shown here) that reflects its lack of robustness to cope with quick and abrupt scintillation fades (e.g. with canonical fades).

B. *Real Data*

The results with the real data are presented in Fig. 9.

For the case of real data it is difficult to plot here the carrier phase error, since there is actually no reference signal we could use as the true and reference carrier to be tracked. In this case, a useful way to proceed is to plot the complex samples at the output of the prompt correlator, as depicted in Fig. 10. Since the carrier phase is being compensated according the corrections imposed by the tracking techniques, we would be expecting the complex prompt samples to represent a binary shift keying constellation. That is, two scatters of points should be centered at values +A and –A, for some value A that encompasses all the scaling factors within the receiver chain.

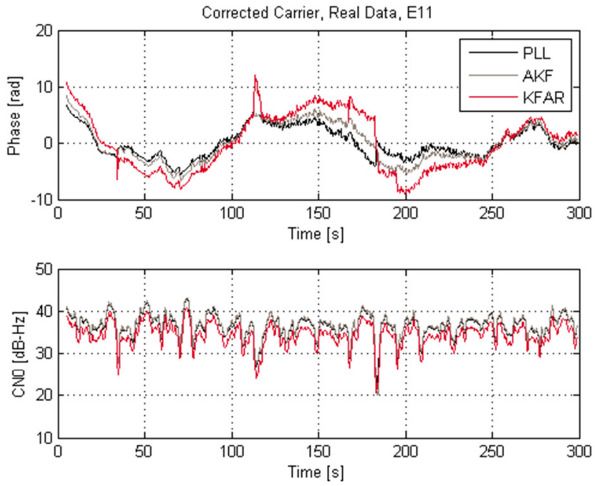

Fig. 9. Results for Galileo, using real data.

This is indeed the result shown in Fig. 10, where the constellation appears fixed (i.e. it does not rotate), which confirms that the signal is being correctly tracked by all techniques. By taking a look at the dispersion of these two scatters, we can have an indication of the actual carrier phase error incurred by the techniques.

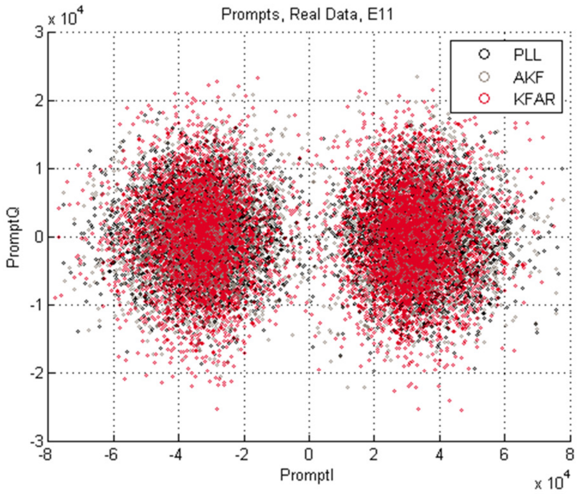

Fig. 10. Data Demodulation Quality Indicator.

At first glance, it can be seen that the largest carrier errors are quite similar in all techniques (i.e. these are the farthest points with respect to the center of the scatter). However, the dots corresponding to the KF-AR are the ones more concentrated around the center of each scatter. The KF-AR is providing the lowest carrier phase variance among all the techniques under analysis. In contrast, the conventional PLL seems to have the largest carrier phase variance, since the corresponding dots have a wider spread with respect to the center of each scatter.

For completeness, the results obtained with the original receiver of the MONITOR project are presented in Fig. 11.

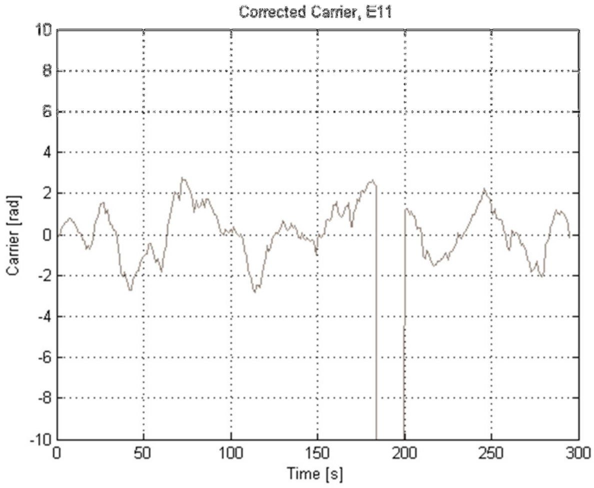

Fig. 11. Results for the same data set with the MONITOR receiver.

The first comment is that the phase is quite similar to the one from the techniques (after unwrapping). Secondly, it can be seen that there is a loss of lock at around 180 seconds (in-line with the strongest signal fade shown in Fig. 7), which is not seen by the robust carrier tracking techniques implemented in our platform. In fact, the loss of lock thresholds of the platform were lowered to 20 dB-Hz and therefore no losses of lock are declared with this signal, even though the phase discontinuities at around 180 seconds are still visible.

C. KF-AR Overview

As detailed in Section II, in addition to tracking the incoming phase, the KF-AR technique aims at estimating the component of the phase variation that can be attributed to the ionospheric scintillations. This allows the KF-AR to separate between the phase component due to the user dynamics and the phase component due to the randomness of the scintillation process. Some results are shown in Fig. 12 to illustrate this separation capability of the KF-AR.

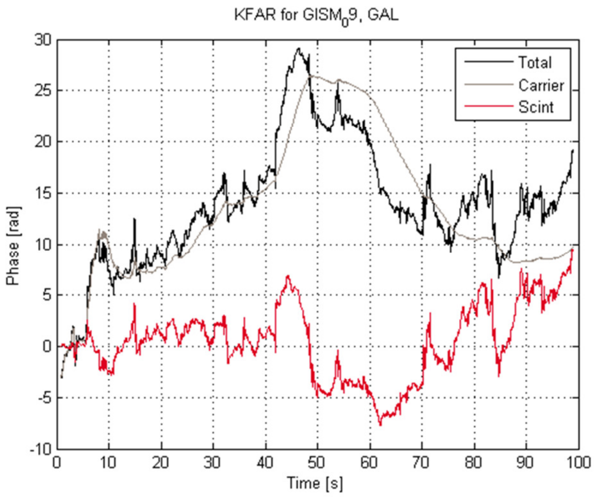

Fig. 12. KF-AR Results for simulated data with S4=0.9.

In Fig. 12, it can be seen that the estimated scintillation component is correctly tracking the shape of phase variations caused by the simulated ionospheric scintillations. It should be noted that the output of these estimated scintillations is wrapped around 2PI to avoid the jumps that appear in the unwrapped estimated phase. These jumps may appear when the input scintillation samples suddenly change (e.g. when the instantaneous S4 parameter exhibits an abrupt increase). In this transition where the stationary behavior of the input scintillation is broken, the scintillation samples momentarily do not fit well in the AR(1) model assumed by the KF-AR. It is for this reason that a transient or glitch may be observed at this point in the estimated scintillation phase, and also some dynamics are introduced by the KF-AR in the total estimated phase to counteract this AR modeling mismatch.

In some sense, this is a normal behavior similar to the one experienced by many signal processing techniques in the presence of outliers or unexpected inputs. Since these events cannot be represented with the actual signal model (which in this case, it is limited to a mere AR(1) process), the KF-AR uses some other variables of the state-space to accommodate this abrupt change in the input signal. In the case under study, this change is inherently modeled by the KF-AR via some non-zero virtual user dynamics that lead to the total estimated phase shown in Fig. 12. Since the scenario being simulated is a static one, there are actually no user dynamics. However, the apparent dynamics estimated by the KF-AR are the way the technique has (with the current configuration) to accommodate abrupt model mismatches. It must be said, though, that this effect can be mitigated through a case-specific tuning of the KF-AR parameters (mainly, the initial covariance and the model noise covariance of the state-space model).

In any case, and after this transient, it is important to remark that the KF-AR is able to track again the input scintillation phase. This can be observed in Fig. 12 by the fact that the shape (i.e. the waveform) of the KF-AR estimated scintillation matches pretty well the one being actually simulated with the GISM model, and originally shown in Fig. 5.

As for the real data, the estimation of the scintillation contribution is presented in Fig. 13.

The results in Fig. 13 are indeed very similar to those provided by the receiver used in the MONITOR project (see Fig. 11). This is particularly true starting at time 60 seconds, and a very similar trend in the estimated scintillation by the KF-AR is preserved until the end of the available data at time 300 seconds. The KF-AR estimated scintillation is apparently a bit more noisy than the one provided by the MONITOR receiver, but this could be mitigated by using some additional moving average at the output, as it is probably done inside the MONITOR receiver. That is to say, there is still some room to further improve the performance of the KF-AR.

Nevertheless, the important point in Fig. 13 is that the proposed KF-AR has been able to overcome the loss of lock that was experienced by the MONITOR receiver in time period from second 180 to 200. The KF-AR was able to keep track, despite the deep fades that were experienced at that time. This example confirms the robustness and potential interest of this innovative KF-AR technique.

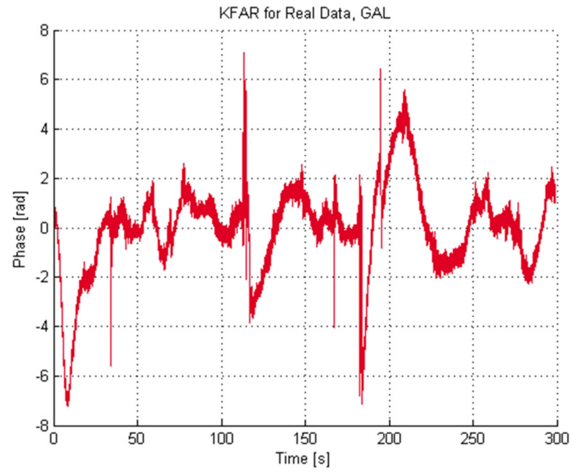

Fig. 13. KF-AR Scintillation estimation from the real data set.

V. CONCLUSIONS

As a conclusion, robust techniques for carrier phase are of paramount importance in trying to maintain tracking of the incoming signal when disturbed by ionospheric scintillations. This study showed that using robust techniques can help smoothing phase transitions, hence potentially pushing back the loss of lock thresholds. Furthermore, it should be noted that the gain in robustness does not entail a loss in accuracy (the resulting jitter is very similar for all techniques). Finally, the phase of the scintillations seemed to be well estimated by all techniques (as far as signal fades take 1-2 seconds in reach their minimum C/N0 value) which is of interest for scientific applications such as ionospheric characterization.

As far as the innovative KF-AR technique is concerned, it has been shown with simulated data that it is able to identify (i.e. to isolate) the phase variations due to scintillations out of the total composite phase. For the real data, the technique seems to also identify fast variations of the phase. Indeed, it is in-line with the reference results provided by the MONITOR receiver, while correctly tracking the overall phase of the incoming signal. As a consequence, not only does this technique increase robustness, but it also provides an estimation of phase variations due to scintillation or at least the effect of similar phenomena which could be used also in integrity applications.

ACKNOWLEDGMENT

Both the simulated and real datasets used for the work presented in this paper have been provided by the European Space Agency. The views presented in the paper represent solely the opinion of the authors and should be considered as research results not strictly related to GALILEO or EGNOS Project design.

REFERENCES

[1] Y. Béniguel, R. Prieto-Cerdeira, et al "Ionospheric Effects on GNSS Performance", Navitec 2012

[2] http://monitor.estec.esa.int/Monitor/

[3] "Ionospheric propagation data and prediction methods required for the design of satellite services and systems", Recommendation ITUR P.531-11, January 2012

[4] Global Positioning System: Theory and Applications", A.J. Van Dierendonck, Volume I, Chapter GPS Receivers, edited by B. Parkinson and J. Spilker Jr, Published by the American Institute of Aeronautics and Astronautics, Inc., 1996.

[5] J. Vilà-Valls, J. A. López-Salcedo, G: Seco-Granados, "An interactive multiple model approach for robust GNSS carrier phase tracking under scintillation conditions", Proc. IEEE Intl. Conf. on Acoustics, Speech and Signal Processing (ICASSP), pp. 6392-6396, May 31 2013.

.